

ISG15 Is Counteracted by Vaccinia Virus E3 Protein and Controls the Proinflammatory Response against Viral Infection

Benedito Eduardo-Correia,^a Carles Martínez-Romero,^{b,d} Adolfo García-Sastre,^{b,c,d} Susana Guerra^a

Department of Preventive Medicine and Public Health and Microbiology, Universidad Autónoma, Madrid, Spain^a; Department of Microbiology^b and Department of Medicine, Division of Infectious Diseases,^c Global Health and Emerging Pathogens Institute,^d Icahn School of Medicine at Mount Sinai, New York, New York, USA

Conjugation of ISG15 inhibits replication of several viruses. Here, using an expression system for assaying human and mouse ISG15 conjugations (ISGylations), we have demonstrated that vaccinia virus E3 protein binds and antagonizes human and mouse ISG15 modification. To study ISGylation importance in poxvirus infection, we used a mouse model that expresses deconjugating proteases. Our results indicate that ISGylation restricts *in vitro* replication of the vaccinia virus VVΔE3L mutant but unconjugated ISG15 is crucial to counteract the inflammatory response produced after VVΔE3L infection.

Type I interferon (alpha/beta interferon [IFN- α/β]) is essential for controlling the replication of viruses in their mammalian hosts. Binding of IFN- α/β to its receptor activates the Janus kinase signal transducer and activator of transcription (JAK/STAT) pathway and consequently leads to the upregulation of hundreds of IFN-stimulated genes (ISG) (1). One of the most highly induced genes is *ISG15*, which encodes a small ubiquitin-like (UBL) protein of 17 kDa that forms covalent conjugates with cellular and viral proteins mediating a considerable antiviral response (2, 3). ISG15 is composed of two domains, each of which carries high sequence and structural similarity to ubiquitin (UB) (33 and 32% for the N- and C-terminal domains, respectively [4]). Conjugation of ISG15 to its protein substrates follows principles similar to those with UB, requiring an E1-activating enzyme (UBE1L), an E2-conjugating enzyme (UbcH8), and an E3 ligase, which in humans is mainly Herc5, while in mice mHerc6 performs this function (5, 6).

The mechanism responsible for the antiviral activity of ISG15 is not clearly understood. ISG15 has been reported to be conjugated to proteins involved in direct or indirect antiviral activity, including RIG-I, JAK1, STAT1, interferon regulatory factor 3 (IRF3), and protein kinase R (PKR) (7, 8). It has also been shown that IRF3 ISG15 conjugation (ISGylation) prevents its ubiquitination and degradation, enhancing its translocation to the nucleus. Consequently, the relative amount of IRF3 is reduced in ISG15^{-/-} cells compared to that in ISG15^{+/+} cells (9). ISG15 negatively regulates important cell signaling pathways, such as RIG-I-like receptor (RLR) signaling and activation of NF- κ B (10, 11). On the other hand, protein de-ISGylation negatively regulates the JAK/STAT pathway (7). It has also been suggested that conjugation of ISG15 to viral proteins has detrimental effects in viral replication. Finally, free, unconjugated ISG15 appear to have antiviral properties, at least for some viruses (12).

Studies with several viruses have verified that ISG15 plays an essential role in the antiviral response (13, 14). Thus, evidence supports the antiviral activity of both conjugated and unconjugated ISG15. For Sindbis virus, the increased lethality seen in ISG15^{-/-} mice can be rescued by a recombinant virus expressing wild-type (WT) ISG15 but not mutant ISG15, the latter not being able to form conjugates *in vitro* (15). In contrast, two reports showed that free ISG15, in the absence of its conjugation cascade, inhibited the release of Ebola virus-like particles (16, 17). Free

ISG15 but not ISGylation promotes antiviral responses against Chikungunya virus infection (12). Previously, we described ISG15 upregulation using cDNA microarrays after infection of HeLa cells with the attenuated vaccinia virus (VACV) strains MVA and NYVAC, an effect not observed after infection with the virulent strain WR (18–20). Also, we have demonstrated the importance of ISG15 in the context of poxvirus infection (21). We evaluated disease progression in ISG15^{-/-} and ISG15^{+/+} mice after infection with WR and with the attenuated mutant VVΔE3L, which lacks the viral early protein E3, using different routes of inoculation. We determined that E3 blocked the antiviral effect of ISG15. However, the mechanism by which E3 is able to block ISG15 is still unknown. The E3 protein also represses the host cell antiviral response by multiple mechanisms, including inhibition of PKR and RNase L, two enzymes induced by IFN. When activated, PKR and RNase L trigger a global inhibition of protein synthesis and of virus replication (22, 23) through the phosphorylation of eIF-2 α (for PKR) and breakdown of RNA (for RNase L). E3 also blocks induction of genes, such as those encoding IFN- α/β , through inhibition of phosphorylation of the transcription factors IRF3 and IRF7 (24, 25) and prevention of NF- κ B activation (26).

Taking into account the important role of ISG15 in establishing the antiviral state of the infected cell, several viruses have developed strategies to counteract its antiviral action. Here, we wanted to investigate if E3 was able to inhibit ISG15 as previously described for the NS1 protein of influenza B virus (27, 28). Influenza B NS1, a protein with structural and functional similarities to E3 (29), binds and inhibits human but not mouse ISG15 (27, 28). Our first approach was to test whether E3 protein was binding to the ISG15 protein of human or mouse origin. Previously, we had described that in the mouse, ISG15 binds the E3 protein in a PKR-independent manner (21). To confirm these results and to extend these studies to the human model, pulldown experiments were performed. For these assays, expression plasmids with glutathione

Received 10 November 2013 Accepted 13 November 2013

Published ahead of print 20 November 2013

Address correspondence to Susana Guerra, susana.guerra@uam.es.

Copyright © 2014, American Society for Microbiology. All Rights Reserved.

doi:10.1128/JVI.03293-13

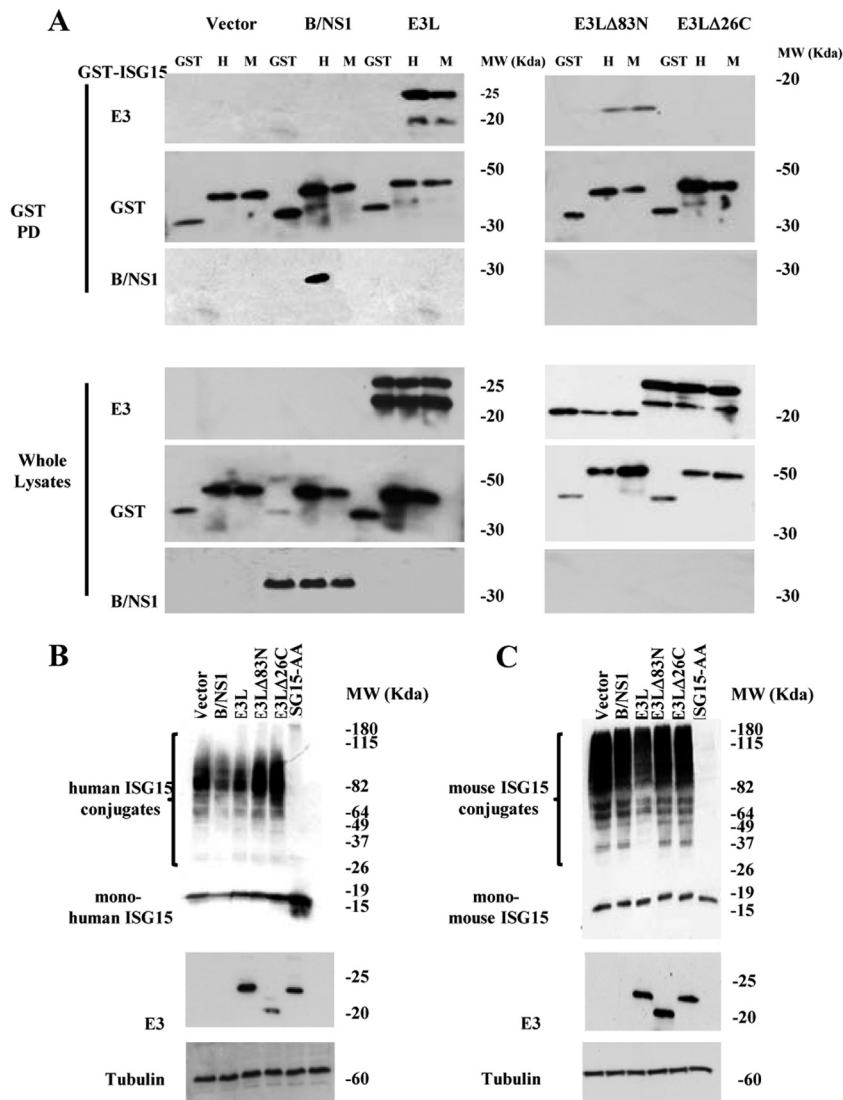


FIG 1 The VACV E3 protein binds to ISG15 from human and murine origin and blocks ISGylation. (A) The C-terminal domain of E3 interacts with human and mouse ISG15. 293T cells were transfected with the indicated plasmids, GST, GST-hISG15 (human origin), or GST-mISG15 (murine origin), and cotransfected with B/NS1 from influenza B/Yamagata/88 virus (Yam88/NS1), the E3 protein from VACV (Western Reserve strain), the last 26 C-terminal amino acids of E3 (VVE3LΔ83N), or the first 83 N-terminal amino acids of E3 (VVE3LΔ26C). Cell lysates were subjected to GST pulldown, and Western blot analysis of precipitated proteins was performed using GST-, NS1/B-, and E3-specific antibodies. Molecular mass markers (kDa) are shown to the right. Three independent experiments were conducted, and a representative image is shown. (B and C) E3 inhibits human and mouse ISGylation. 293T cells were transfected with the indicated plasmids, and then 24 h later, cell lysates were analyzed by Western blotting for V5-ISG15 conjugation using a V5 tag-specific antibody. The expression of the different E3 domains was analyzed by Western blotting using a specific antibody against E3. Tubulin was used as loading control. (B) Human E1, E2, E3, and V5-hISG15 plasmids were cotransfected with plasmids encoding B/NS1 or E3 protein from VACV (WR strain), either with the last 26 C-terminal amino acids of E3 (VVE3LΔ83N) or with the first 83 N-terminal amino acids of E3 (VVE3LΔ26C). The concentration of conjugation machinery plasmids was kept constant, while the relative amounts of hISG15 plasmid were lowered and hISG15 was replaced by B/NS1. In the line indicated as ISG15-AA, a control of nonconjugated ISG15 (v5-hISG15-AA) was transfected with human E1, E2, and E3. Three independent experiments were performed, and a representative image is shown. (C) Murine E1, E2, E3, and V5-hISG15 plasmids were cotransfected with plasmids encoding B/NS1 or E3, either with the last 26 C-terminal amino acids of E3 or with the first 83 N-terminal amino acids of E3. In the line indicated as ISG15-AA, a control of nonconjugated ISG15 (v5-mISG15-AA) was transfected with murine E1, E2, and E3. Three independent experiments were performed, and a representative image is shown.

S-transferase (GST) fused in frame to human or mouse ISG15 were generated and coexpressed in 293T cells with plasmids encoding the entire viral E3 gene or B/NS1, which was used as a control. Protein lysates were subjected to GST pull-down, and precipitated proteins were analyzed by Western blotting using E3-, NS1-, and GST-specific antibodies (Fig. 1, left panels). In the whole-cell lysates (Fig. 1A, lower-left panels), similar expression

levels of E3 and GST fusions were observed. In both cases, GST-hISG15 and GST-mISG15 precipitated with E3 (Fig. 1A, upper-left panels), indicating that E3 is able to interact with human and also murine ISG15. E3 has two domains: an N-terminal domain, involved in the direct inhibition of the IFN-induced double-stranded RNA (dsRNA)-dependent protein kinase PKR in nuclear localization and in Z-DNA binding (30–32), and a C-terminal

domain, which contains the dsRNA-binding domain required for IFN resistance and for the broad-host-range phenotype of the virus (30, 33). To study whether the specific region responsible for the binding between the E3 protein and ISG15 was the same in the murine and human systems, we constructed plasmids expressing two portions of the E3 protein: the first was 165 amino acids in length and the last was 108 amino acids. We then performed similar pulldown experiments using the two portions of the E3 protein. The C-terminal domain of E3 is needed for its interaction with murine or human ISG15 (Fig. 1A, right panels). These results indicate that VACV E3 has a higher binding permissibility for ISG15 from multiple species than B/NS1, because differences between mouse and human ISG15 sequence are not influencing E3 protein binding ability. However, substituting the mouse sequence (QNCSE) for the human hinge sequence (DKCDE) in human ISG15 resulted in a total loss of NS1B binding (34).

ISGylation) to substrate proteins occurs in a manner similar to that of UB conjugation, by utilizing activating, conjugating, and ligating enzymes to facilitate the addition of ISG15 to specific lysine residues. Although we defined that E3 regulates ISG15 activity, the only evidence until now that suggests that E3 blocks the ISGylation process is the increased level of ISGylated complexes observed in VVΔE3L-infected mouse lung homogenates (21). To elucidate whether E3 blocks ISGylation activity and to further gain insights into its mechanism, we performed an *in vitro* assay that allowed us to study the impact of the expression of E3 on protein ISGylation. We transfected 293 cells with ISG15 and its specific E1 (UBE1), E2 (UbcM8), and E3 (HERC5) enzyme expression plasmids to evaluate ISGylated protein levels in both human and murine systems. Next, we compared levels of ISGylated protein after cotransfection of the E3 plasmid with the plasmids described above. Using the human ISGylation system, we observed a decrease in total ISGylation when E3 was coexpressed. This suggests that E3 might be blocking the ISGylation activity of human ISG15 (Fig. 1B). When we performed similar experiments using the murine system, we also observed a decrease in the ISGylation levels when the entire E3 VACV protein was cotransfected, although the efficacy of this blockage is lower than that observed in the human system (Fig. 1C). Interestingly, both C- and N-terminal domains of E3 are required for ISGylation inhibition, indicating that E3 binding to ISG15 is not sufficient for ISGylation inhibition.

Host restriction of a virus is driven by its ability to counteract specific components of the innate immune response in selected species. In the context of influenza B virus, its inability to block ISGylation in mice and in other hosts as well may contribute to limiting the host range of the virus. Moreover, it might account for the increased susceptibility of ISG15^{-/-} mice to influenza virus infection, as previously described (35). In contrast, the capacity of VACV to counteract ISGylation by E3 in the murine system correlated with a lack of differences in pathogenesis between ISG15^{-/-} and ISG15^{+/+} cells infected with VACV, as we previously reported (21).

According to the aforementioned considerations, we can speculate that subversion of ISGylation may control virus replication in mouse infection. In order to elucidate this question and to define the roles between ISG15 and ISGylation in the context of VACV infection, we used a transgenic mouse model in which proteases with deconjugating activity (OTU) are expressed (36). Therefore, although ISG15 is expressed, ISGylation is completely repressed. We have previously reported that the attenuated

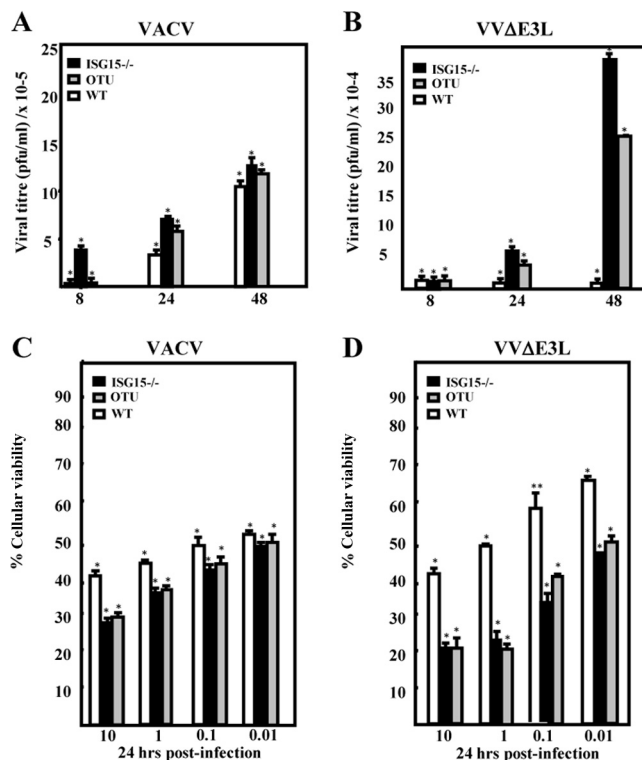


FIG 2 Effect of ISG15 and ISGylation on virus growth and cytotoxicity after infection of MEFs with VACV or VVΔE3L viruses. (A) ISG15^{-/-}, out, or ISG15^{+/+} mice were mock infected or infected at 0.1 PFU/cell with VACV (WR) or VVΔE3L. At different times postinfection, cells were harvested and virus yields were determined by plaque assay for VACV or by immunostaining for VVΔE3L. (B) Cellular viability of ISG15^{-/-}, out, or ISG15^{+/+} cells infected with VACV (WR) or VVΔE3L virus at the indicated multiplicity of infection (MOI) from 0.01 to 10 PFU/cell. Twenty-four hours postinfection (hpi), the medium was removed and cytotoxicity was determined by crystal violet staining. The percentage of viable cells after infection was calculated assuming the survival rate of uninfected cells to be 100%. Three independent experiments were carried out, and a representative experiment is shown. Error bars indicate the standard deviations of the means. Student's *t* test was performed to determine the *P* value. (**, *P* < 0.05; *, *P* < 0.01).

VVΔE3L virus was able to grow in ISG15^{-/-} mouse embryonic fibroblasts (MEFs) (21). Our next step was to understand if this phenotype was also observed in OTU MEFs. The cytopathic effect (CPE) observed in OTU MEFs after VACV (WR strain) infection (0.1 PFU/cell, 24 h) was similar to that with ISG15^{-/-} or ISG15^{+/+} cells (data not shown). However, the CPE after VVΔE3L infection in OTU cells was similar to that in ISG15^{-/-} cells and was markedly increased compared to that observed in ISG15^{+/+} cells (data not shown). VACV viral titers were slightly increased in ISG15^{-/-} and OTU cells compared to those in ISG15^{+/+} cells (Fig. 2A). On the other hand, a significant increase of VVΔE3L yields was observed in ISG15^{-/-} and OTU cells compared to results for ISG15^{+/+} cells (Fig. 2B). In the VVΔE3L-infected ISG15^{-/-} and OTU cells, the increase in virus titers correlated with increase in cellular mortality (Fig. 2D), indicating that VVΔE3L overcomes viral growth blockage only in the absence of ISGylation. This suggests that E3-mediated ISGylation inhibition might account for similar levels in VACV replication in ISG15^{-/-} ISG15^{+/+} or OTU cells, thus validating our *in vitro* assays shown in Fig. 1.

To expand these studies to an *in vivo* model, transgenic OTU and wild-type mice were inoculated intranasally with different doses of VACV (WR strain). We examined the degree of viral pathogenesis during the first days of the infection, and no differences in weight loss and in mortality were detected between OTU and wild-type mice (Fig. 3A). Although at the higher dose of VACV, all OTU transgenic animals died, while the WT animals were still alive, we do not think these are significant differences, since 2 days later, all the WT infected animals also succumbed to infection. This result indicates that there were no differences in pathogenesis with VACV-infected ISG15^{-/-} or OTU mice in comparison to that with ISG15^{+/+} mice. However, in the case of VVΔE3L, an enhanced inflammatory response and mortality are observed only after ISG15^{-/-} high-dose infection (21). To analyze whether the cause of VVΔE3L-associated increased pathogenicity in infected ISG15^{-/-} mice was due to a lack of ISGylation, we infected OTU transgenic mice with VVΔE3L virus. OTU, ISG15^{-/-}, and ISG15^{+/+} mice were inoculated intranasally with 10⁸ PFU of VVΔE3L per mouse, and weight loss and mortality were evaluated. As previously described (21), VVΔE3L-infected ISG15^{-/-} mice displayed mild disease symptoms within 3 days, and 25% of them died at 1 day postinfection (dpi) after a high dose in the absence of viral replication in the lungs (Fig. 3B). Surprisingly, when ISGylation was decreased due to the expression of the OTU transgene, VVΔE3L was still attenuated (Fig. 3). The animals also displayed mild signs of disease at 3 dpi, but all the animals recovered at the endpoint of the experiment (Fig. 3B). Also, VVΔE3L virus could not be detected in lung lysates from either OTU, ISG15^{-/-}, nor ISG15^{+/+} animals (Fig. 3C). This result suggests that the presence of unconjugated ISG15, which is not affected in the OTU transgenic mouse, is a requirement to maintain the attenuated phenotype of VVΔE3L virus *in vivo* (Fig. 3A and B). Histological examination of lung tissues at 1 dpi showed that ISG15^{+/+} or OTU animals infected with VVΔE3L virus had no inflammatory cells infiltrating the lung parenchyma. In contrast, lung sections obtained from VVΔE3L-infected ISG15^{-/-} mice presented a severe inflammation pattern, with alveolar wall thickening and infiltration of inflammatory cells (Fig. 4A). Lung inflammation was also drastically reduced in infected OTU mice. These results suggest that unconjugated ISG15 is responsible for counteracting the development of an exacerbated inflammatory response after a high dose of VVΔE3L virus. To analyze the state of ISGylation in the VACV- or VVΔE3L-infected mice, lungs were homogenized and ISG15 levels were determined by Western blotting. While ISG15^{-/-} mice do not express ISG15 (Fig. 4B), lungs from OTU mice showed only unconjugated ISG15, as expected, whereas the homogenates from ISG15^{+/+} mice showed free ISG15 and ISG15 conjugated to cellular targets (Fig. 4B). The conjugation of ISG15 to its targets proteins was considerably enhanced in lung extracts from mice infected with VVΔE3L in comparison to those infected with VACV. This result suggests that E3 also was able to inhibit the ISGylation *in vivo*, validating our *in vitro* analysis (Fig. 1). Since the inflammatory response might explain the rapid signs of illness in high-dose VVΔE3L-infected ISG15^{-/-} mice, we measured serum cytokine levels (interleukin 6 [IL-6], tumor necrosis factor alpha [TNF-α], IL-10, monocyte chemoattractant protein 1, IFN-γ, and IL-12 p70) at early times postinfection in the infected ISG15^{-/-}, ISG15^{+/+}, or OTU mice. IL-6 levels were very low and were similar in serum from VVΔE3L-infected OTU or ISG15^{+/+} animals (Fig. 4C). In contrast, ISG15^{-/-} mice

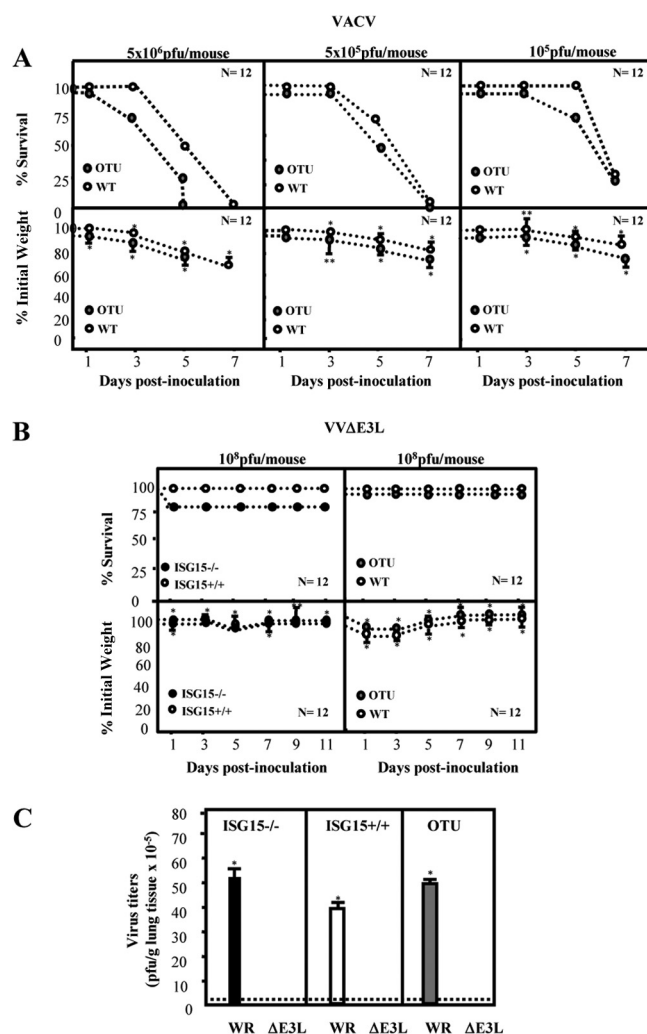


FIG 3 A decrease in the ISGylation levels does not vary VACV pathogenesis. (A) Transgenic OTU (ISGylation deficient; gray circles) or wild-type (white circles) mice were infected intranasally with 10⁵, 5 × 10⁵, or 5 × 10⁶ PFU/mouse of VACV (WR strain). Infected mice were weighed daily, and the mean percentage weight loss of each group ($n = 12$) was compared with the weight immediately before the infection (lower panels). The upper panels show the survival rate. Two independent experiments were carried out, and a representative experiment is shown. Error bars indicate the standard deviations of the means. Student's *t* test was performed to determine the *P* value. (**, $P < 0.05$; *, $P < 0.01$). (B) VVΔE3L infection is attenuated in the OTU mice. ISG15^{-/-} (black circles), transgenic OTU (gray circles), or WT (white circles) mice were infected by the intranasal route with 10⁸ PFU/mouse. Infected mice were weighed individually daily, and the mean percentage weight loss of each group ($n = 12$) was compared with the weight immediately prior to infection (lower panels). The upper panels show the survival rate. Two independent experiments were carried out, and a representative experiment is shown. Error bars indicate the standard deviations of the means. Student's *t* test was performed to determine the *P* value. (**, $P < 0.05$; *, $P < 0.01$). (C) Viral replication of different VACV strains in infected ISG15^{+/+}, ISG15^{-/-}, and OTU mice. At 24 hpi, lung homogenates were titrated by plaque assay in BSC40 (for WR) or by immunostaining in BHK-21 cells (for VVΔE3L). Three independent experiments were carried out, and a representative experiment is shown. Results represent the means ± SD for individual samples of 6 mice/day/group. Student's *t* test was performed to determine the *P* value. (*, $P < 0.01$). The dotted line represented the detection limit.

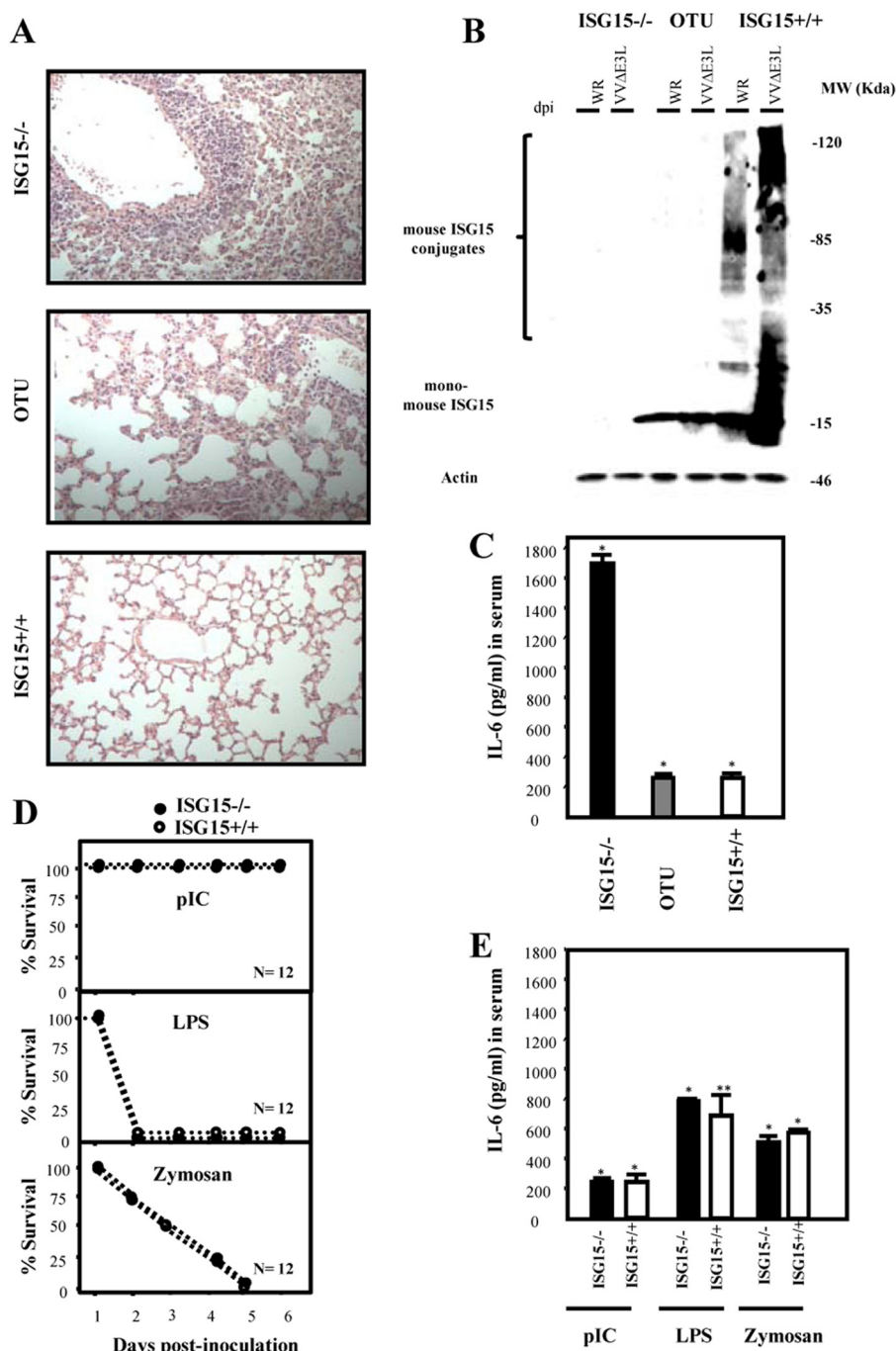


FIG 4 Free ISG15 is essential for controlling the proinflammatory response after infection of VVΔE3L. (A) Histopathology of lungs from ISG15^{-/-}, OTU, and ISG15^{+/+} mice intranasally infected with VVΔE3L (10^8 PFU/mouse). At 24 hpi, infected lungs were resected, sectioned, and stained with hematoxylin and eosin. Three independent experiments were performed, using 3 animals each, for each group of animals. Representative fields of the 9 histology specimens analyzed are shown at a magnification of $\times 100$. (B) Western blot of ISG15 in lung homogenates from ISG15^{-/-}, OTU, and ISG15^{+/+} mice intranasally infected for 24 h with VACV or VVΔE3L (10^8 PFU/mouse). Each sample represents pools from 6 mice per group. On the right, the molecular masses of the proteins (in kilodaltons) are indicated. Actin levels showed that the same amounts of protein were loaded on the gel. Three independent experiments were carried out, and a representative image is shown. (C) IL-6 levels in serum of ISG15^{-/-} (black bars), OTU (gray bars), or WT (white bars) mice infected with VVΔE3L (10^8 PFU/mouse) were measured by enzyme-linked immunosorbent assay (ELISA) from serum collected at 3 hpi. Three independent experiments were carried out, and a representative experiment is shown. Each result represents the mean \pm SD for pooled samples from 6 mice. Student's *t* test was performed to determine the *P* value (*, *P* < 0.01). (D) ISG15^{-/-} and ISG15^{+/+} mice were inoculated intraperitoneally with poly(I:C) (10 mg/kg), LPS (15 mg/kg), and zymosan (15 mg/kg), and the survival curves of all the groups (*n* = 12) were represented. Two independent experiments were carried out, and results of a representative experiment are shown. (E) IL-6 levels in serum of ISG15^{-/-} (black bars) or WT (white bars) mice inoculated intraperitoneally with poly(I:C) (10 mg/kg), LPS (15 mg/kg), and zymosan (15 mg/kg) were measured by ELISA from serum collected at 3 hpi. Three independent experiments were carried out, and results of a representative experiment are shown. Results represent the means \pm SD for pooled samples from 6 mice. Student's *t* test was performed to determine the *P* value (**, *P* < 0.05; *, *P* < 0.01).

infected with VVΔE3L showed an 8-fold increase in serum levels of IL-6 compared to those for ISG15^{+/+} or OTU infected mice ($P < 0.01$) (Fig. 4C). There were no changes in levels of other cytokines analyzed between the groups (not shown). Cytokine and chemokine release occurs rapidly in response to virus infection, with the aim of recruiting inflammatory leukocytes in order to limit virus replication and spread and to induce adaptive immunity. However, prolonged expression of chemokines in the context of viral infections may be detrimental to the host, provoking the so-called cytokine storm. Here, we demonstrated that in the absence of nonconjugated ISG15, VVΔE3L infection produces an increase of IL-6 that correlates with short-term morbidity and complications that include pulmonary function abnormalities, indicating that free ISG15 might be involved in the downregulation of IL-6 induction, facilitating a balanced, nonpathogenic innate immune response. To verify that the morbidity was induced by VVΔE3L infection, we evaluated the survival rate of ISG15^{-/-} and ISG15^{+/+} mice inoculated with different inflammatory agents, such as poly(I:C) (10 mg/kg), lipopolysaccharide (LPS) (15 mg/kg), and zymosan (15 mg/kg) (Fig. 4D). In all cases, the survival kinetics was similar between the two types of mice and no differences in the IL-6 levels in the serum of the treated mice were observed (Fig. 4E). This result indicates that VVΔE3L infection was the cause of the mortality and also caused exacerbated levels of IL-6 in ISG15^{-/-} mice. Whether these effects are due to the absence of E3 directly or to another process, the mechanisms of this ISG15-dependent, ISGylation-independent regulation remain to be determined, but it appears that ISG15 controls the antiviral response in multiple ways, depending on whether it is or is not conjugated. Also, it is important to underscore that free ISG15 becomes secreted and the lack of secreted ISG15 is associated with severe mycobacterial disease in both mice and humans (37). Furthermore, we recently reported the importance of ISG15 in regulating macrophage activity (38), indicating that ISG15 is a crucial molecule in the regulation of the immune response. Additional studies to understand the biological functions of unconjugated intracellular and/or extracellular ISG15 and of ISGylation may help our knowledge of innate immunity and on how viruses have developed strategies to subvert it.

ACKNOWLEDGMENTS

We thank Gijs Versteeg for his help in the *in vitro* transfection experiments, Klaus-Peter Knobeloch, Skip Virgin, and Debbie Lenschow for sharing the ISG15^{-/-} and OTU transgenic animals, and Beltram L. Jacobs for the generous gift of the VVΔE3L deletion mutant and the rabbit E3 antibody. We also thank Beatriz Martín, Richard Cadagan, and Osman Lizardo for excellent technical assistance.

This work was supported by grants from the Spanish Ministry of Health, FIS2011-00127, and UAM-Banco de Santander to S.G. and was also partly supported by NIAID grant U19AI083025 to A.G.-S.

REFERENCES

1. Diamond MS, Farzan M. 2013. The broad-spectrum antiviral functions of IFIT and IFITM proteins. *Nat. Rev. Immunol.* 13:46–57. <http://dx.doi.org/10.1038/nri3344>.
2. Au WC, Moore PA, Lowther W, Juang YT, Pitha PM. 1995. Identification of a member of the interferon regulatory factor family that binds to the interferon-stimulated response element and activates expression of interferon-induced genes. *Proc. Natl. Acad. Sci. U. S. A.* 92:11657–11661. <http://dx.doi.org/10.1073/pnas.92.25.11657>.
3. Austin KJ, Bany BM, Belden EL, Rempel LA, Cross JC, Hansen TR. 2003. Interferon-stimulated gene-15 (ISG15) expression is up-regulated in the mouse uterus in response to the implanting conceptus. *Endocrinology* 144:3107–3113. <http://dx.doi.org/10.1210/en.2002-0031>.
4. Liu YC, Penninger J, Karin M. 2005. Immunity by ubiquitylation: a reversible process of modification. *Nat. Rev. Immunol.* 5:941–952. <http://dx.doi.org/10.1038/nri1731>.
5. Dastur A, Beaudenon S, Kelley M, Krug RM, Huibregtse JM. 2006. Herc5, an interferon-induced HECT E3 enzyme, is required for conjugation of ISG15 in human cells. *J. Biol. Chem.* 281:4334–4338. <http://dx.doi.org/10.1074/jbc.M512830200>.
6. Zhao C, Beaudenon SL, Kelley ML, Waddell MB, Yuan W, Schulman BA, Huibregtse JM, Krug RM. 2004. The UbcH8 ubiquitin E2 enzyme is also the E2 enzyme for ISG15, an IFN- α /beta-induced ubiquitin-like protein. *Proc. Natl. Acad. Sci. U. S. A.* 101:7578–7582. <http://dx.doi.org/10.1073/pnas.0402528101>.
7. Malakhova OA, Yan M, Malakhov MP, Yuan Y, Ritchie KJ, Kim KI, Peterson LF, Shuai K, Zhang DE. 2003. Protein ISGylation modulates the JAK-STAT signaling pathway. *Genes Dev.* 17:455–460. <http://dx.doi.org/10.1101/gad.1056303>.
8. Zou W, Papov V, Malakhova O, Kim KI, Dao C, Li J, Zhang DE. 2005. ISG15 modification of ubiquitin E2 Ubc13 disrupts its ability to form thioester bond with ubiquitin. *Biochem. Biophys. Res. Commun.* 336:61–68. <http://dx.doi.org/10.1016/j.bbrc.2005.08.038>.
9. Lu G, Reinert JT, Pitha-Rowe I, Okumura A, Kellum M, Knobeloch KP, Hassel B, Pitha PM. 2006. ISG15 enhances the innate antiviral response by inhibition of IRF-3 degradation. *Cell. Mol. Biol. (Noisy-le-Grand)* 52: 29–41.
10. Kim MJ, Hwang SY, Imaizumi T, Yoo JY. 2008. Negative feedback regulation of RIG-I-mediated antiviral signaling by interferon-induced ISG15 conjugation. *J. Virol.* 82:1474–1483. <http://dx.doi.org/10.1128/JVI.01650-07>.
11. Minakawa M, Sone T, Takeuchi T, Yokosawa H. 2008. Regulation of the nuclear factor (NF)- κ B pathway by ISGylation. *Biol. Pharm. Bull.* 31:2223–2227. <http://dx.doi.org/10.1248/bpb.31.2223>.
12. Werneke SW, Schilte C, Rohatgi A, Monte KJ, Michault A, Arenzana-Seisdedos F, Vanlandingham DL, Higgs S, Fontanet A, Albert ML, Lenschow DJ. 2011. ISG15 is critical in the control of Chikungunya virus infection independent of UBE1L mediated conjugation. *PLoS Pathog.* 7:e1002322. <http://dx.doi.org/10.1371/journal.ppat.1002322>.
13. Lenschow DJ. 2010. Antiviral properties of ISG15. *Viruses* 2:2154–2168. <http://dx.doi.org/10.3390/v2102154>.
14. Skaug B, Chen ZJ. 2010. Emerging role of ISG15 in antiviral immunity. *Cell* 143:187–190. <http://dx.doi.org/10.1016/j.cell.2010.09.033>.
15. Lenschow DJ, Giannakopoulos NV, Gunn LJ, Johnston C, O'Guin AK, Schmidt RE, Levine B, and Virgin HW, IV. 2005. Identification of interferon-stimulated gene 15 as an antiviral molecule during Sindbis virus infection in vivo. *J. Virol.* 79:13974–13983. <http://dx.doi.org/10.1128/JVI.79.22.13974-13983.2005>.
16. Malakhova OA, Zhang DE. 2008. ISG15 inhibits Nedd4 ubiquitin E3 activity and enhances the innate antiviral response. *J. Biol. Chem.* 283: 8783–8787. <http://dx.doi.org/10.1074/jbc.C800030200>.
17. Okumura A, Pitha PM, Harty RN. 2008. ISG15 inhibits Ebola VP40 VLP budding in an L-domain-dependent manner by blocking Nedd4 ligase activity. *Proc. Natl. Acad. Sci. U. S. A.* 105:3974–3979. <http://dx.doi.org/10.1073/pnas.0710629105>.
18. Guerra S, Lopez-Fernandez LA, Conde R, Pascual-Montano A, Harshman K, Esteban M. 2004. Microarray analysis reveals characteristic changes of host cell gene expression in response to attenuated modified vaccinia virus Ankara infection of human HeLa cells. *J. Virol.* 78:5820–5834. <http://dx.doi.org/10.1128/JVI.78.11.5820-5834.2004>.
19. Guerra S, Lopez-Fernandez LA, Pascual-Montano A, Munoz M, Harshman K, Esteban M. 2003. Cellular gene expression survey of vaccinia virus infection of human HeLa cells. *J. Virol.* 77:6493–6506. <http://dx.doi.org/10.1128/JVI.77.11.6493-6506.2003>.
20. Guerra S, Lopez-Fernandez LA, Pascual-Montano A, Najera JL, Zaballos A, Esteban M. 2006. Host response to the attenuated poxvirus vector NYVAC: upregulation of apoptotic genes and NF- κ B-responsive genes in infected HeLa cells. *J. Virol.* 80:985–998. <http://dx.doi.org/10.1128/JVI.80.2.985-998.2006>.
21. Guerra S, Caceres A, Knobeloch KP, Horak I, Esteban M. 2008. Vaccinia virus E3 protein prevents the antiviral action of ISG15. *PLoS Pathog.* 4:e1000096. <http://dx.doi.org/10.1371/journal.ppat.1000096>.
22. Rivas C, Gil J, Melkova Z, Esteban M, Diaz-Guerra M. 1998. Vaccinia virus E3L protein is an inhibitor of the interferon (i.f.n.)-induced 2-5A

- synthetase enzyme. *Virology* 243:406–414. <http://dx.doi.org/10.1006/viro.1998.9072>.
23. Wreschner DH, Silverman RH, James TC, Gilbert CS, Kerr IM. 1982. Affinity labelling and characterization of the ppp(A2'p)nA-dependent endoribonuclease from different mammalian sources. *Eur. J. Biochem.* 124: 261–268.
 24. Smith EJ, Marie I, Prakash A, Garcia-Sastre A, Levy DE. 2001. IRF3 and IRF7 phosphorylation in virus-infected cells does not require double-stranded RNA-dependent protein kinase R or Ikappa B kinase but is blocked by Vaccinia virus E3L protein. *J. Biol. Chem.* 276:8951–8957. <http://dx.doi.org/10.1074/jbc.M008717200>.
 25. Xiang Y, Condit RC, Vijaysri S, Jacobs B, Williams BR, Silverman RH. 2002. Blockade of interferon induction and action by the E3L double-stranded RNA binding proteins of vaccinia virus. *J. Virol.* 76:5251–5259. <http://dx.doi.org/10.1128/JVI.76.10.5251-5259.2002>.
 26. Deng L, Dai P, Ding W, Granstein RD, Shuman S. 2006. Vaccinia virus infection attenuates innate immune responses and antigen presentation by epidermal dendritic cells. *J. Virol.* 80:9977–9987. <http://dx.doi.org/10.1128/JVI.00354-06>.
 27. Sridharan H, Zhao C, Krug RM. 2010. Species specificity of the NS1 protein of influenza B virus: NS1 binds only human and non-human primate ubiquitin-like ISG15 proteins. *J. Biol. Chem.* 285:7852–7856. <http://dx.doi.org/10.1074/jbc.C109.095703>.
 28. Versteeg GA, Hale BG, van Boheemen S, Wolff T, Lenschow DJ, Garcia-Sastre A. 2010. Species-specific antagonism of host ISGylation by the influenza B virus NS1 protein. *J. Virol.* 84:5423–5430. <http://dx.doi.org/10.1128/JVI.02395-09>.
 29. Guerra S, Abaitua F, Martinez-Sobrido L, Esteban M, Garcia-Sastre A, Rodriguez D. 2011. Host-range restriction of vaccinia virus E3L deletion mutant can be overcome in vitro, but not in vivo, by expression of the influenza virus NS1 protein. *PLoS One* 6:e28677. <http://dx.doi.org/10.1371/journal.pone.0028677>.
 30. Chang HW, Jacobs BL. 1993. Identification of a conserved motif that is necessary for binding of the vaccinia virus E3L gene products to double-stranded RNA. *Virology* 194:537–547. <http://dx.doi.org/10.1006/viro.1993.1292>.
 31. Kim YG, Muralinath M, Brandt T, Percy M, Hauns K, Lowenhaupt K, Jacobs BL, Rich A. 2003. A role for Z-DNA binding in vaccinia virus pathogenesis. *Proc. Natl. Acad. Sci. U. S. A.* 100:6974–6979. <http://dx.doi.org/10.1073/pnas.0431131100>.
 32. Langland JO, Jacobs BL. 2004. Inhibition of PKR by vaccinia virus: role of the N- and C-terminal domains of E3L. *Virology* 324:419–429. <http://dx.doi.org/10.1016/j.virol.2004.03.012>.
 33. Beattie E, Kauffman EB, Martinez H, Perkus ME, Jacobs BL, Paoletti E, Tartaglia J. 1996. Host-range restriction of vaccinia virus E3L-specific deletion mutants. *Virus Genes* 12:89–94. <http://dx.doi.org/10.1007/BF00370005>.
 34. Yin C, Khan JA, Swapna GV, Ertekin A, Krug RM, Tong L, Montelione GT. 2007. Conserved surface features form the double-stranded RNA binding site of non-structural protein 1 (NS1) from influenza A and B viruses. *J. Biol. Chem.* 282:20584–20592. <http://dx.doi.org/10.1074/jbc.M611619200>.
 35. Lenschow DJ, Lai C, Frias-Staheli N, Giannakopoulos NV, Lutz A, Wolff T, Osiak A, Levine B, Schmidt RE, Garcia-Sastre A, Leib DA, Pekosz A, Knobeloch KP, Horak I, Virgin HW, IV. 2007. IFN-stimulated gene 15 functions as a critical antiviral molecule against influenza, herpes, and Sindbis viruses. *Proc. Natl. Acad. Sci. U. S. A.* 104:1371–1376. <http://dx.doi.org/10.1073/pnas.0607038104>.
 36. Frias-Staheli N, Giannakopoulos NV, Kikkert M, Taylor SL, Bridgen A, Paragas J, Richt JA, Rowland RR, Schmaljohn CS, Lenschow DJ, Snijder EJ, Garcia-Sastre A, Virgin HW, IV. 2007. Ovarian tumor domain-containing viral proteases evade ubiquitin- and ISG15-dependent innate immune responses. *Cell Host Microbe* 2:404–416. <http://dx.doi.org/10.1016/j.chom.2007.09.014>.
 37. Bogunovic D, Byun M, Durfee LA, Abhyankar A, Sanal O, Mansouri D, Salem S, Radovanovic I, Grant AV, Adimi P, Mansouri N, Okada S, Bryant VL, Kong XF, Kreins A, Velez MM, Boisson B, Khalilzadeh S, Ozcelik U, Darazam IA, Schoggins JW, Rice CM, Al-Muhsen S, Behr M, Vogt G, Puel A, Bustamante J, Gros P, Huibregtse JM, Abel L, Boisson-Dupuis S, Casanova JL. 2012. Mycobacterial disease and impaired IFN-gamma immunity in humans with inherited ISG15 deficiency. *Science* 337:1684–1688. <http://dx.doi.org/10.1126/science.1224026>.
 38. Yanguéz E, Garcia-Culebras A, Frau A, Llompart C, Knobeloch KP, Gutierrez-Erlandsson S, Garcia-Sastre A, Esteban M, Nieto A, Guerra S. 2013. ISG15 regulates peritoneal macrophages functionality against viral infection. *PLoS Pathog.* 9:e1003632. <http://dx.doi.org/10.1371/journal.ppat.1003632>.